PII: S0955-2219(98)00091-0

0955-2219/98/$— see front matter

# Processing Character of MgO-Partially Stabilized Zirconia (PSZ) in Size Grading Prepared by Injection Molding

Wen-Cheng J. Wei* and Yuh-Pring Lin

Tjing Ling Industrial Research Institute, National Taiwan University, Taipei, 106 Taiwan

(Received 24 November 1997; revised version received 5 March 1998; accepted 11 March 1998)

***Abstract***

*The effects of the mixture of coarse/fine $ZrO_2$ powders in various ratios on the properties of injection-molding feedstocks, the degree of debinding, dimension reproducibility, sintering and phase formation of the Mg-partially stabilized zirconia (PSZ) were studied. The feedstocks and injection molded pieces with 3·5 wt% MgO were tested by capillary rheometry, thermal analysis (DSC), and the injection-molded pieces were analyzed by mercury porosimetry, Archimedes' method. After sintered, the density and m-phase were analyzed by SEM and quantitative XRD techniques. Experimental results show when the feedstocks contained ≥50 vol% of coarse powder, the viscosity is lower and the activation energies of the feedstocks are in the same range as that of pure binder admixture. The flowing properties are controlled by the ratio of fine to coarse as the concentration of fine powder was over 50 vol%. In addition, the formulations with a higher content in fine powder would enhance the de-polymerization of PP, improve the dimensional reproducibility, homogeneity, and degree of debinding. With the appropriate controls on the ratio of fine to coarse powders, Mg–PSZ with 60 to 93% theoretical density and uniform microstructure can be produced.* 

## 1 Introduction

Zirconia is a well-known high temperature material. A high melting point, a low thermal conductivity, a thermal expansion coefficient close to iron-based materials, and good resistance to slag attack, make zirconia a good refractory. However, two disadvantages, namely high cost and poor-to-fair thermal shock resistance, limit the high temperature applications of zirconia. A tundish nozzle[1–3] for steelmaking is one of the widely used applications of $ZrO_2$ refractory.

Size grading is a useful method for the improvement of refractory resistance to thermal shock. Coarse granules are currently used as part of the refractory formulation. The amount of coarse fraction may be as high as 40%.[4] Nevertheless, the densification of the refractory is subsequently retarded and results in a porous body. The porosity is beneficial for arresting or deflecting cracks at the stage of fracturing, which also improves the shock resistance of the refractory. However, the strength and resistance of the refractory to slag corrosion are degraded dramatically if the porosity is abundant and interconnected. That is due to the porosity of the refractory cannot resist the penetration of slag during metal processing at high temperatures.

In addition to the size grading, a recent research work on a series of composites with a duplex microstructure is reported by Lutz *et al.*[5] They reported that improvement of thermal shock can be obtained from crack deflection and branching by a reinforcing second phase. A homogeneous distribution of reinforcing, secondary phase is the primary characteristic of the composites.

Injection molding (IM) is one of the interesting processing techniques of the past two decades for making fine ceramics. These ceramics, including alumina, zirconia and silicon nitride, are fabricated by this technique for high performance applications, such as ceramic turbines or cutting tools. The technique offers the opportunity for mass production of ceramic parts with complicated shapes combined with the advantages of dimensional

*To whom correspondence should be addressed.

reproducibility and near-net-shape formation. However, only Ce- and Y-doped zirconia specimens are at present reported using this shaping technique.[6–10] The mechanical properties of zirconia made by injection molding are close to or higher[9] than those made by other techniques. It is worthwhile to investigate the zirconia system, Mg-partially stabilized zirconia (PSZ), which is often used as a refractory material, in order to understand the advantages and differences of parts made from this material by injection molding.

An improved refractory with well-distributed fine/coarse grains and a designed microstructure is desirable for the applications of the $ZrO_2$ refractory in high value products.[3] A fundamental knowledge is needed to clearly identify the roles of size grading and the fine/coarse powder admixtures. The factors of microstructural homogeneity which influences the mechanical properties and the performance of thermal shock will be mentioned in another paper.[11] In this study, a fixed binder composition and solid loading in the feedstocks were followed through in this study. Therefore, the flow properties of the plastic feedstocks and the variation of injection molded parts were studied with an emphasis on the effects of fine to coarse ratio of the zirconia powders. The homogeneity of feedstocks and injection molded pieces was also investigated by using different analytical techniques. The study would help to find the key factors and to understand the advantages and disadvantages of the precision injection molding process.

## 2 Experimental

### 2.1 Materials

Two zirconia powders and one MgO powder were used for the preparation of the PSZ mixture. One is coarse and MgO stabilized powder (AQZ-100, Universal Abrasives, UK) in an average particle size of 60 $\mu$m. The other is the fine monoclinic (m) phase powder (non-stabilized, EF-PREMIUM, Z-Tech Co., USA) in an average particle size of 1 $\mu$m. The properties of the zirconia powders are listed in Table 1. A phase stabilizer MgO was prepared from the calcination of a high purity hydrolyzed magnesium carbonate powder [$Mg_5(CO_3)_4(OH)_25H_2O$, City Gate International Co., Ltd., ROC]. The powder mixtures were formulated as indicated in Table 2 to keep a constant MgO content of 3·5 wt%.

The binder system contained PP (Polypropylene, Taiwan Polypropylene Co., ROC), PW (Paraffin Wax, Nacalai Teque Inc., Japan), and SAM (Magnesium Stearic Acid, Hayashi Pure Chemical Industries Ltd., Japan) which was used as a plasticizer. Due to the complexity of the binder formulation, only one binder composition with a fixed ratio of three ingredients was used (Table 2). In addition to the composition of the binder, Table 2 also depicts the codes for five formulations of which the binder loadings were kept at 50 vol%. In other words, the solid loading was fixed at 50 vol%. However, the flowing properties, which will be reported later, of all the feedstocks are not identical. Therefore, the injection molding conditions also reported in Table 2 were adjusted according to the viscosity of each feedstock at the shear rate of 1000 $s^{-1}$. The injection temperature was gradually increased from 150 to 210°C as the content of the fine powder increased.

**Table 1.** Composition and properties of zirconia powders

| *Powder Property* | | *AQZ* | *EF* |
|---|---|---|---|
| Particle size (d50) ($\mu$m) | | 60·1 | 1·0 |
| Density (g $cm^{-3}$) | | 5·65 | 4·73 |
| Composition (wt%) | $ZrO_2 + HfO_2$* | 95·40 | 99·33 |
| | CaO | 0·30 | 0·04 |
| | Mgo | 3·66 | 0·01 |
| | $Fe_2O_3$ | 0·12 | 0·03 |
| | $TiO_2$ | 0·15 | 0·07 |
| | $SiO_2$ | 0·30 | 0·28 |
| | Other | 0·07 | 0·24 |

*The content of $HfO_2$ is 1–2 wt%.

### 2.2 Processing of feedstocks and injection molding

Plastic feedstocks were prepared using a Σ-type kneader operated with a constant rotation rate of 35 rpm. The details of mixing sequence of each compound are indicated in Lin's thesis.[12] Samples were injection-molded by the equipment (CDC9000 SM50 injection molder, Chen-Hsong Machinery Taiwan, Co., Ltd.). Then the samples were solvent-debinded using n-heptane ($C_7H_{10}$) operated at 40 to 60°C for 3 h. A thermal debinding was then conducted on the solvent-debinded specimens as follows:

a heating rate 2°C $min^{-1}$ to 250°C, dwelling for 2 h at 250°C;
raising to 400°C, dwelling for 10 min at 400°C;
a heating rate of 5°C $min^{-1}$ to 1000°C, dwelling for 10 min at 1000°C.

After debinding, the samples were sintered at the temperatures of 1450–1750°C at a heating rate of 10°C $min^{-1}$ in a 1800°C high temperature furnace (Lindberg, a General Signal Co., USA).

### 2.3 Characterization

Well-mixed plastic mixtures (called 'feedstocks') were tested by capillary rheometry (self-constructed[12]), thermal analysis (DSC-50, Shimadzu

**Table 2.** Composition and injection conditions of five zirconia mixtures

| *Symbol* | *Powder* (total in 50 vol%)* | | | | *Injection molding conditions* | | |
|---|---|---|---|---|---|---|---|
| | *AQZ (wt%)* | *EF (wt%)* | *Added MgO (wt%)* | *Total of MgO (wt%)* | *Molding temperature (°C)* | *Molding pressure (MPa)* | *Molding rate (cc $s^{-1}$)* |
| F00 | 100 | 0 | 0 | 3·5 | 150 | 95·7 | 25·6 |
| F25 | 75 | 25 | 0·88 | 3·5 | 170 | 95·7 | 25·6 |
| F50 | 50 | 50 | 1·75 | 3·5 | 190 | 95·7 | 25·6 |
| F75 | 25 | 75 | 2·63 | 3·5 | 210 | 95·7 | 25·6 |
| F100 | 0 | 100 | 3·50 | 3·5 | 210 | 95·7 | 32 |

*The solid loading of all formulations is kept at 50 vol%. The contents of PP, PW and SAM in the formulation are 12·5, 35 and 2·5 wt%, respectively.

Co., Japan) and mercury porosimetry (Autopore II 9220, Micromeritics Instrument Co., USA) to investigate the viscosity of feedstocks, the degree of solvent debinding and thermal debinding and the pore size distribution of IM parts.

The rheometer used a set of three capillary molds in which the pressure difference ($\Delta P$) as a function of capillary diameter/length (R/L) was calibrated before the viscosity measurement. In addition, the Rabinowitsch corrections[13] were used to calculate the real shear rate ($\gamma_w$) on the wall of capillary and the apparent viscosity ($\eta$) of the non-Newtonian feedstocks.

A scanning electron microscope (Mini-SEM, Jeol Co., Japan) was used to observe the fracture surface of the IM parts in three stages. After sintering, the density of zirconia was measured by the Archimedes' method. The amount of monoclinic phase in the as-sintered zirconia was determined by a quantitative XRD technique reported by Garvie *et al.*[14]

## 3 Results and Discussion

### 3.1 Flowing properties of feedstocks

Figure 1 shows the viscosity of the F50 feedstock (50% coarse + 50% fine powder) and pure binder (25% PP + 70% PW + 5% SAM) measured by a capillary rheometer operated at different shear rates. The viscosity of the F50 and the binder was dependent on the testing temperature. Noting that the binder was tested between 130 and 150°C (i.e. 20°C in average lower than the feedstock), the binder should have a lower value than the viscosity of any feedstocks containing 50 vol% zirconia powder.

The viscosity of each feedstock is dependent on the formulation of powder mixtures and the temperature, as show in Fig. 2. For a greater volume fraction of coarse particles, the surface area of the powder mixture is smaller. The interaction between the coarse particles and the binder is less in F00 than that in the F100. As a consequence, the flowing at a lower temperature is easier for these

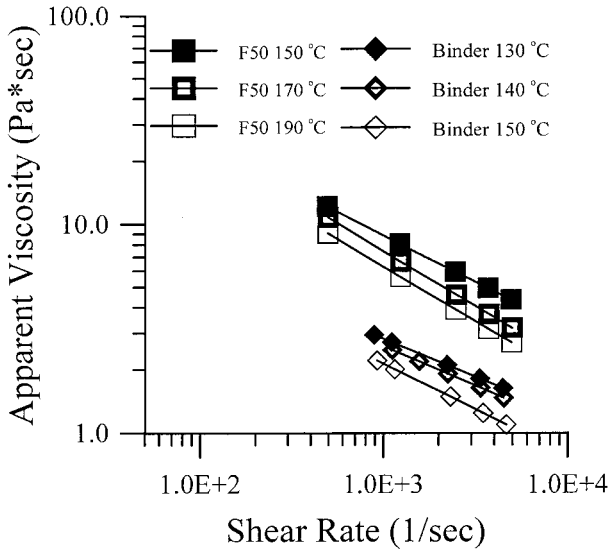


**Fig. 1.** Apparent viscosity of F50 feedstocks and pure binder.

formulations, e.g. F25 or F00, than F100. Since the binder in this study has the same formulation (solid loading) and ingredient in all feedstocks, the variation of the viscosity of the feedstocks is mainly due to the size grading of the PSZ powders.

The rheology of the powder/plastic mixture has been studied.[15] The solid loading, ratio of large/small particles, and the aspect ratio of powder shape were characterized as a function of relative viscosity of the mixture. Chong *et al.*[15] report that the viscosity shows a minimum at 30 to 40% volume content of small particles. That is different from the flow behavior of the PSZ feedstocks shown in Fig. 2 which behave a gradually decrease in viscosity as the increase of the fine PSZ content. In fact, the particles Chong used were spherical glass beads with a smooth surface. The spherical beads are also larger in diameter than the fine PSZ powder used in this study. The submicrometric PSZ powder behaves a stronger surface force which is distinct from glass beads. Accordingly, the fine PSZ particles do not just locate in the interstitial sites of large particles, but also interact with viscous polymer at injection molding temperature. The fine PSZ particles indeed dominate the flow behavior of the feedstocks.

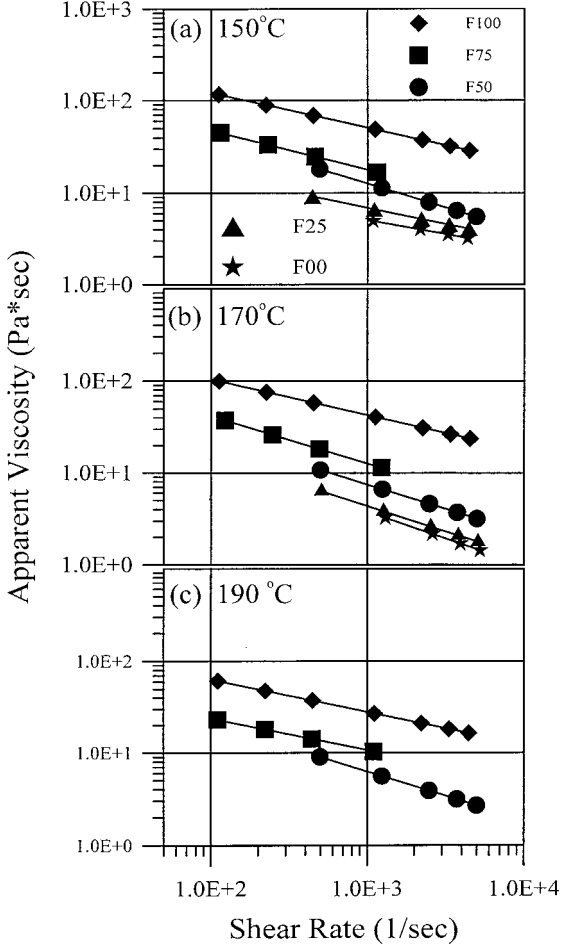


**Fig. 2.** Apparent viscosity of five feedstocks tested at temperatures either at 150, 170 or 190°C.

The dependence of viscosity ($\eta$) on the shear rate ($\gamma$) can be fitted by:

$$\eta = k(\gamma)^{n-1} \text{ or } \ln\eta = \ln k + (n-1)\ln\gamma \qquad (1)$$

where $k$ is the viscosity parameter (or consistency index), and $n$ is the flow index of plastic flow. The data are shown in Fig. 2. Table 3 shows the results of the flow index ($n$) and viscosity parameter ($k$) of the feedstocks and the binder tested at different temperatures. The value of $n$ ranges from 0·45 to 0·78 and has a standard deviation of ca. 10%. The $n$ values fall within the $n$ values, range from 0·27 to 0·70, of various $Al_2O_3$ feedstocks reported in the literature.[16–18] In our previous investigation,[16] it was shown that the mixing conditions (e.g. homogeneity of an admixture and mixing sequence) for the preparation of feedstocks strongly influences the $n$ values. The higher the testing temperature, the closer the $n$ value to unity. The repeatability of $n$ is good for homogeneous feedstocks. Due to the scattering of the values in Table 3 and previous reasons, it is hard to compare the $n$ values between different feedstocks. From the $n$ values of all feedstocks it only can be concluded to be close to 0·5 and lower than 1·0, indicating that the flow behavior is pseudoplastic in the temperature range considered.

**Table 3.** Flow index ($n$) and viscosity parameter ($k$, Pa $s^{-1}$) of five compositions and pure binder measured at various temperatures

| *Temperature (°C)* | *F100* | *F75* | *F50* | *F25* | *F00* | *Pure binder* |
|---|---|---|---|---|---|---|
| 130 | | | | | | 0·63<br>36 |
| 140 | | | | | | 0·62<br>36 |
| 150 | 0·63<br>679 | 0·57<br>340 | 0·48<br>194 | 0·64<br>79 | 0·68<br>46 | 0·57<br>43 |
| 160 | | | | 0·59 | 0·61<br>92 | 72 |
| 170 | 0·61<br>623 | 0·48<br>448 | 0·47<br>278 | 0·46<br>224 | 0·45<br>197 | |
| 190 | 0·64<br>332 | 0·66<br>116 | 0·47<br>237 | | | |
| 210 | 0·78<br>105 | 0·55<br>143 | | | | |
| 230 | 0·63<br>155 | | | | | |

*The values reported in the table are in the form of $\frac{n}{k}$.

The viscosity parameter ($k$), which represents the viscosity at zero shear rate, of the five feedstocks and pure binder is also listed in Table 3. The $k$ values have a standard deviation of ca. 20%. But interesting trends are found in Table 3. In fine-powder formulations (e.g. F100 and F75), the higher the temperature, the lower the $k$ value. However, the formulations F00 and F25 with coarse powder perform differently. They (F00 and F25) have a higher $k$ value at a higher temperature. In addition, the $k$-value increases with increasing volume fraction of fine powder.

Figure 3 is a plot of the data points of the apparent viscosity measured at a shear rate of 1000 $s^{-1}$. The variation of viscosity with respect to the temperature revealed that the flow behavior was largely controlled by the addition of fine powders, in other words, by the ratio of the fine/coarse fraction in the formulations. The fitted lines in Fig. 3 represent the temperature dependence of the viscosity. Those are fitted as the Arrhenius' equation.

$$\eta = \eta_0 \exp\left(-\frac{E}{RT}\right) \text{ or } \ln\eta = \ln\eta_0 - \left(\frac{E}{R}\right)\frac{1}{T} \qquad (2)$$

where the activation energy $E$ (kJ $mol^{-1}$) of a plastic flow is equal to the value of ($R{\cdot}m$), in which $R$ is the gas constant and $m$ is the slope of the fitted lines in Fig. 3. The values and the deviation of the activation energy in Fig. 3 were also estimated and reported in Fig. 4. The activation energy of F50, F25 or F00 is in the range of 13–17 kJ $mol^{-1}$, nearly

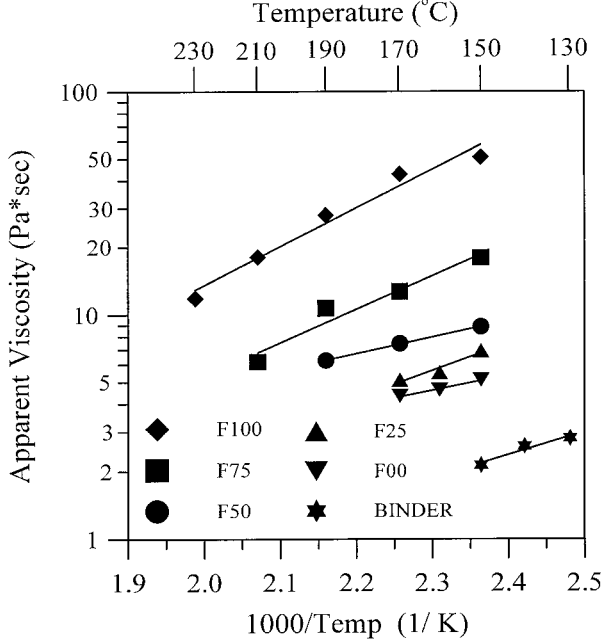


**Fig. 3.** Apparent viscosity of five feedstocks measured at constant shear rate ($10^3\,s^{-1}$).

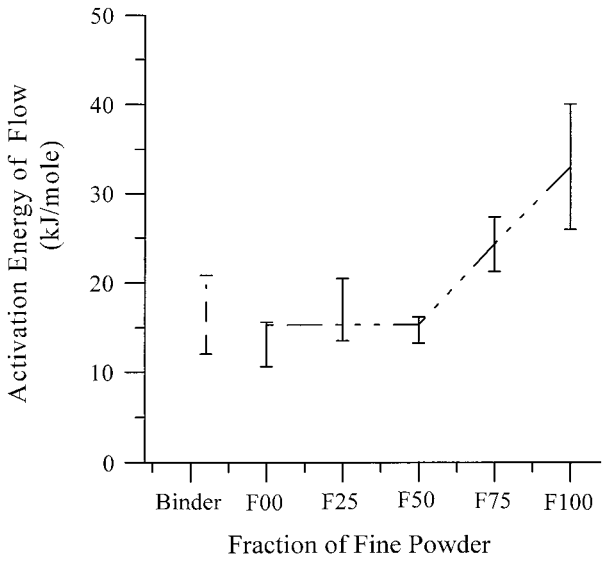


**Fig. 4.** Activation energies of five feedstocks and pure binder.

the same as the $E$ value ($16{\cdot}4 \pm 3{\cdot}6\,kJ\,mol^{-1}$) of the pure binder. But the $E$ values of previous formulations are smaller than those of F75 and F100. The 50% concentration of the fine powder seems to be a critical amount on the change of the activation energy for the PSZ feedstocks.

The activation energy increases linearly for a fine powder content of more than 50%, as shown in Fig. 4. It is assumed that the plastic layer between the particles above this value is too thin for the material to flow as a bulky binder system. The interaction of fine particles (EF–zirconia) dominates as the volume fraction of the fine powder is more than 50%. Therefore, the solid loading of the fine powder should be critical for the dependence of the flowing of feedstocks on the temperature.

### 3.2 Degradation of feedstocks

It was noted that the high molecular PP melted above 140°C and fibrous texture would appear as the PP and ceramic powder were kneaded together. During the kneading, high shear forces were acting on the powder and binder ingredients, causing the ceramic powder to de-agglomerate and also forced the PP to de-polymerize. The more the surface of powder is exposed to binder, the more the binder degraded.

A DSC analysis of the degradation of binder was conducted to reveal the interaction of PSZ particles and the influence on the binder. F100 and F00 feedstocks were kneaded under the same procedures. The DSC results of the two feedstocks are shown in Fig. 5. The curves show three decomposition peaks (41·7, 57 and 140·5°C) in the low temperature region. Our previous study[16] on the PP/PW/SA (stearic acid) binder system has shown that the endothermic peaks at 41·7 and 57·0°C are the melting points of PW, and the peak at 140·5°C belongs to the melting of PP. In the present system, the thermal reactions of SAM are probably too small to be detected due to the low concentration of SAM. At higher temperatures (more than 200°C), F100 and F00 show also the same decomposition (probably a moderate oxidation), but the number and positions of the exothermic peaks are very different. There are exothermic peaks at 211·9, 266·2 and 348·9°C in F100, representing three possible ranges of exothermic reactions of the residue decomposed at various temperatures. But there is only one broad peak starting from 160°C and one greater exothermic peak at 331·4°C in F00. The F00 shows a moderate exothermic reaction starting at 160°C and then extensive reaction above 300°C. However, there is one peak more in F100 than that of F00, implying that some of the PP in F100 is readily de-polymerized by the shearing effects exerted from the fine EF–$ZrO_2$ powder. Therefore, the Mw distribution of PP in F100 becomes wider after the kneading step and its decomposition is extended over a wider temperature range.

The degradation may have two effects on the feedstocks. One is that the viscosity of the F100 should be lower due to a lower average molecular weight of PP. However, the increments in the viscosity from the influence of fine powder surface are dominating. The apparent viscosity of F100 is in fact higher than F00 (Fig. 2).

The second effect can be seen from the appearance of the fractured surface of debinded F00, which contains a fibrous remainder [Fig. 6(e)]. Figure 6 shows the fractured surfaces of F100 and F00 at different processing stages, after injection molding, after solvent or after thermal debinding. These fibrous features are not found in F100. The

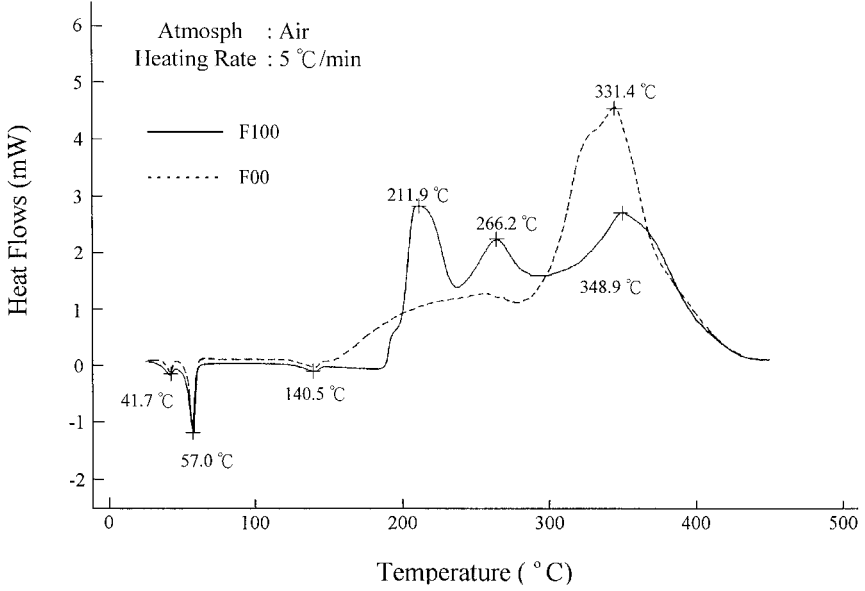


**Fig. 5.** DSC histograms of F00 and F100 feedstocks.

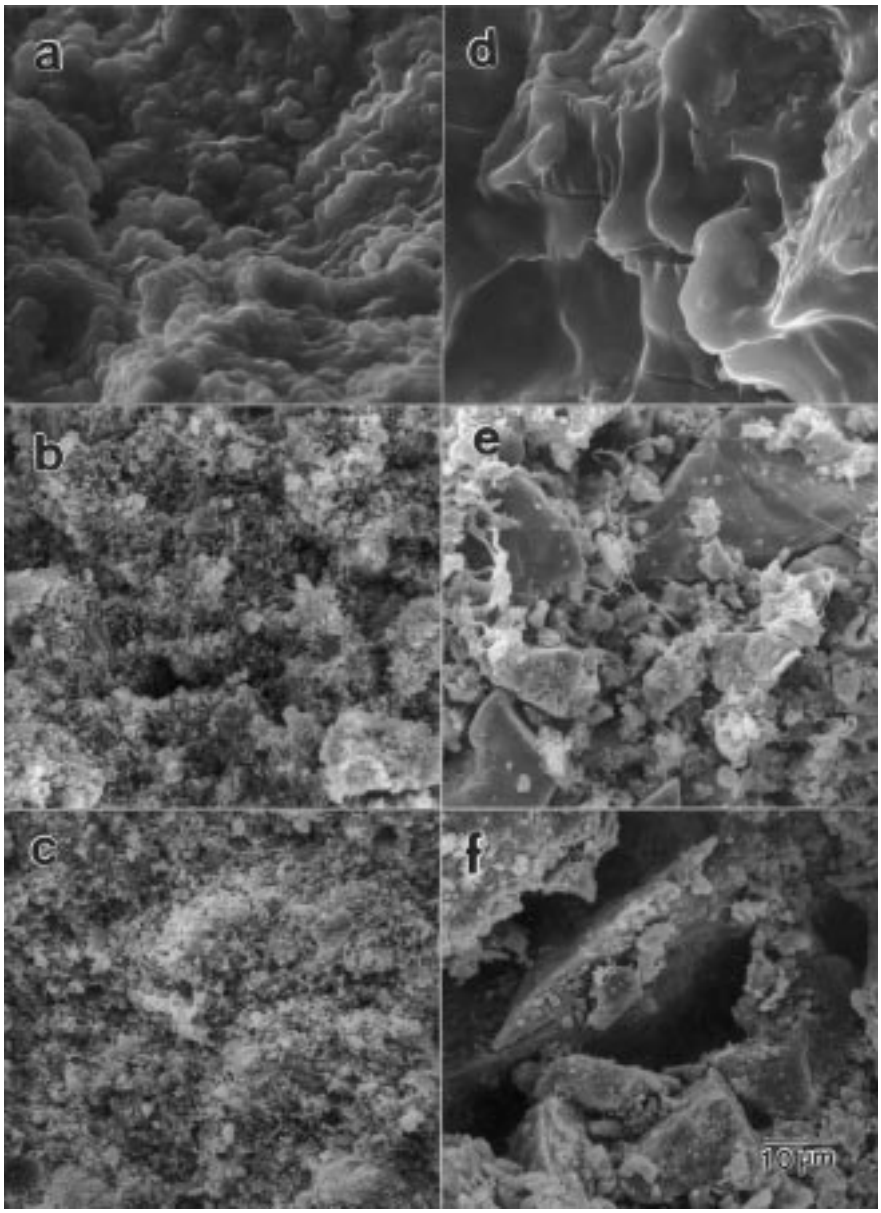


**Fig. 6.** SEM micrographs of the fracture surfaces of (a) as-injection molded part, (b) solvent debinded and (c) thermal debinded parts of F100; (d) as-injection molded parts, (e) solvent debinded, and (f) thermal debinded parts of F00.

enhancement of the PP degradation by fine $ZrO_2$ powder and the dominance of the fine powder on the flow behavior are obvious.

### 3.3 Properties of injection molded parts

The injection molding conditions, including molding temperature, pressure and molding rate, were selected according to the variation of the viscosity of each of the feedstocks. The molding temperature, as shown in Table 2, is the major variable in the shape forming step. The temperature changes from 150 to 210°C as the content of fine powder increases.

The bulk density of molded specimens was measured and shown in Fig. 7. The bulk density of the formulations F00 and F25 is higher than those F75 and F100 with a large content of fine powder. The variation of bulk density can be reduced to less than 2%* if the fine powder in the formulation is more than 50%. The higher the fine powder content, the narrower the density variation.

Figure 6(a) and (d) shows SEM micrographs of as-molded F100 and F00. The ceramic powder is covered by the polymeric materials and appears granular in texture corresponding to the size of $ZrO_2$. After solvent debinding, the surface of the ceramic powder is exposed as depicted in Fig. 6(b) and (e). During which no PP is identified from Fig. 6(b) and (e) except for some PP fibers remaining in the powder matrix.

The specimens were solvent-debinded in *n*-heptane at various solvent temperatures, either 40, 50, or 60°C. The results shown in Fig. 8 reveal that the curves of the weight loss of the five samples are hardly distinguishable. The amount of dissolved binder (PW and SAM) after 3 h treatment is in the range of 65 to 67% which is less than the content (75%) of PW + SAM.

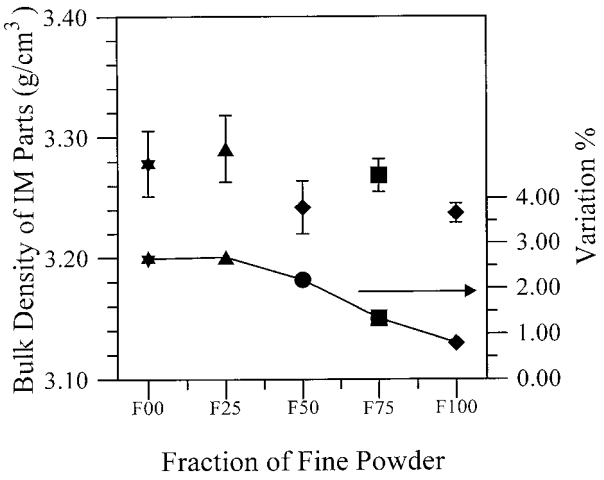


**Fig. 7.** Bulk density and density variation (%) of IM parts plotted against the fraction of fine powder.

*This is the variation generally acceptable in ceramic injection molding industry.

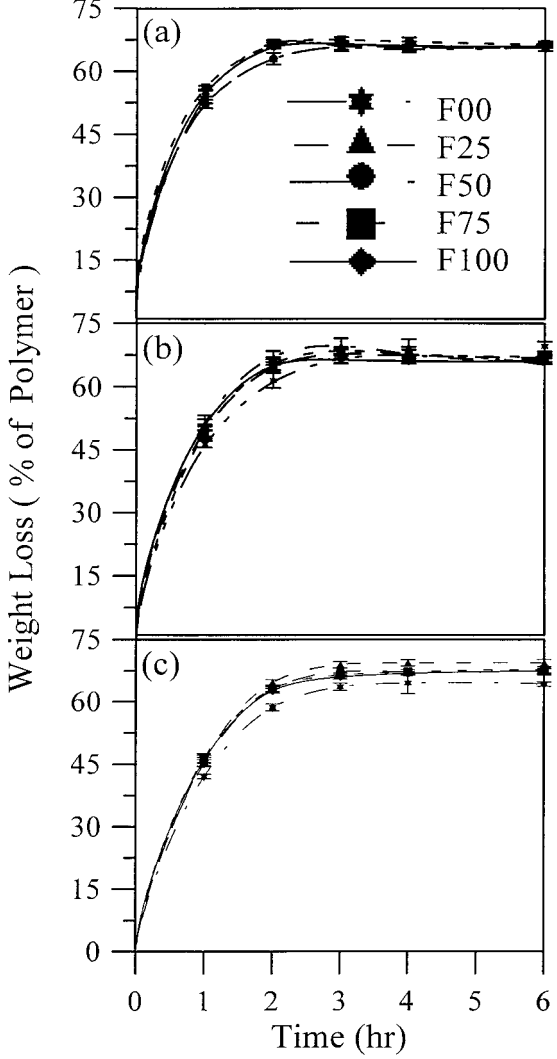


**Fig. 8.** Weight loss of injection molded parts after solvent debinding for various periods and solvent temperatures of (a) 60, (b) 50 and (c) 40°C.

The degree of debinding by solvent and thermal treatments is shown in Fig. 9. The variation of the solvent debinding of the compositions F00 and F25 containing more coarse powder is greater than that of either F75 or F100 (Fig. 9). The trend in the variation is also observed for thermal debinding. In fact, the debinding is not complete for the compositions F00 and F25. That is an average of 2·5% of the binder either remained in the samples or was lost before the injection molding. The low-temperature ingredients, such as PW or SAM, may lose 1 to 2% during kneading in an open chamber or may incompletely pyrolyze to form any stable carbon phase during thermal debinding. Another possibility is that the surface of the coarse powder induces less uniformity in the thermally debinding effect. Therefore, the PP residue in the sample is result. The variation and amount of the debinding of F00 and F25 are not as good as in the other cases.

After solvent debinding (60°C for 3 h) and thermal debinding, the pore size distribution of the five

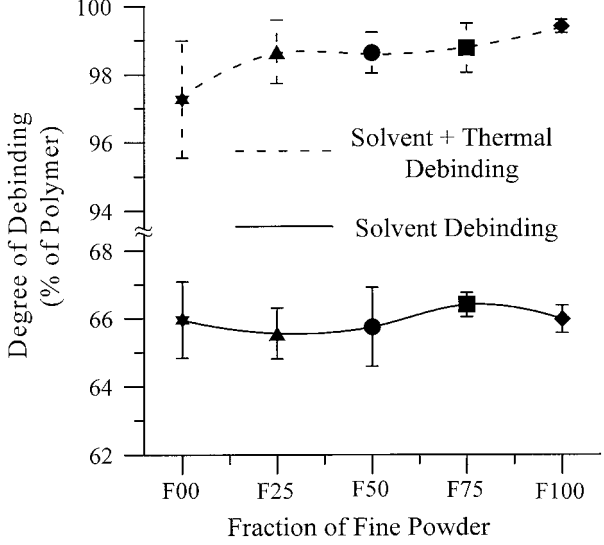


**Fig. 9.** Degree of solvent debinding and thermal debinding as a function of fine powder in zirconia formulation.

samples through these two steps was measured and shown in Fig. 10. In solvent debinding stage, there appears a broad distribution in pore size, ranging over 2 orders of magnitude. The smallest size of the open pores is around 0·01 $\mu$m, formed by the dissolution of the soluble ingredients, PW and SAM. The pore size distribution of the samples after thermal debinding is much narrower than that after solvent debinding. The porosity of the thermally debinded samples is a normal distribution. The pore size of the samples corresponds to the interstitial space between the zirconia particles of each composition. This can be seen from the micrographs of thermally debinded samples shown in Fig. 6(c) and (f) where the pore size of F100 and F00 corresponds to the particle size and similar to those in the stage of solvent debinding.

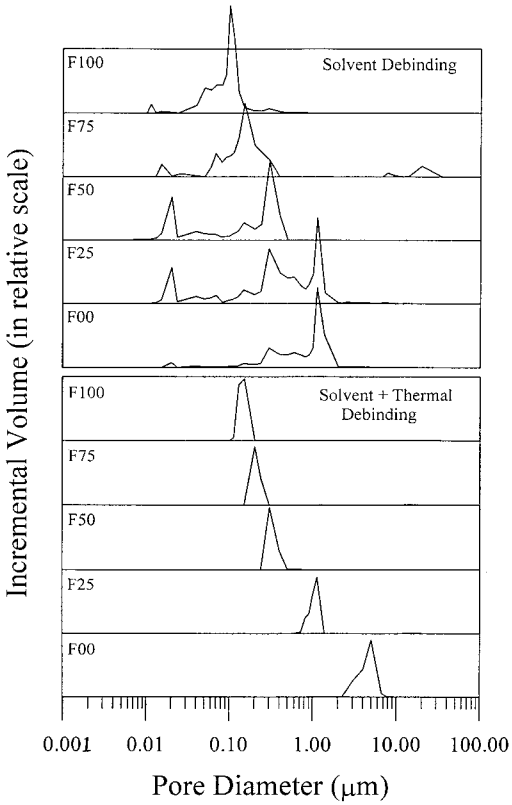


**Fig. 10.** Size distribution of porosity of the injection molded specimens after solvent debinding (60°C for 3 h) and thermal debinding treatments.

### 3.4 Densification and crystalline phase of IM zirconia

Figure 11(a) shows the bulk density of the F50 zirconia sintered at 1450–1750°C using various times. The data show that the density can be improved only marginally if the sintering temperature of F50 is increased from 1650 to 1750°C. However, the sintered density increases appreciably if the ratio of the fine/coarse powder of the formulation increases, as shown in Fig. 11(b). The F100 batches have the highest density of 5·25 g $cm^{-3}$, which is equal to 93% of the theoretical density. It is also noted from Fig. 11(a) and (b) that the sintering of each batch is nearly complete after 1 h at any temperature higher than 1550°C. This is a special characteristic of the zirconia prepared from the mixtures with a majority of the content being coarse powder.

The samples sintered at 1650°C for 1 h were quantitatively analyzed by XRD and the results are shown in Fig. 12. There are monoclinic (m), tetragonal (t) and cubic (c) phases of the zirconia indexed in the patterns of Fig. 12(a). The X-ray spectra of five samples show clean zirconia phases and no MgO. The amount of monoclinic phase is analyzed by using the diffraction peaks between 27 to 33° two-theta angle, as shown in Fig. 12(b). The

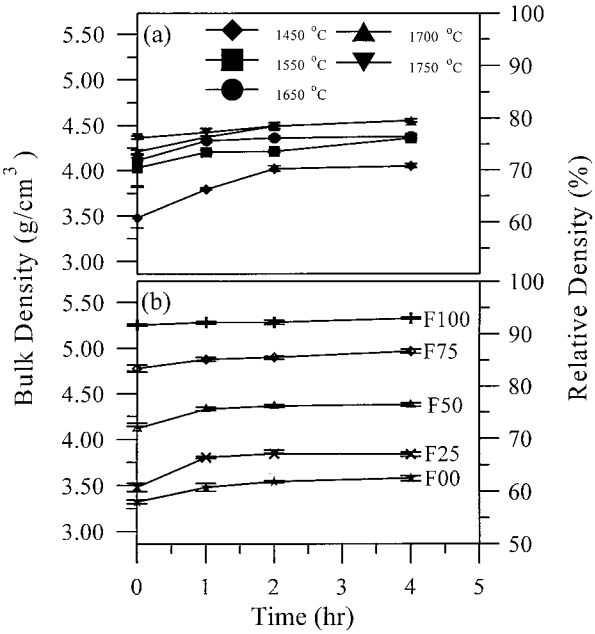


**Fig. 11.** Sintered density and porosity of (a) F50 at different temperatures and (b) five compositions fired at 1650°C for different times.

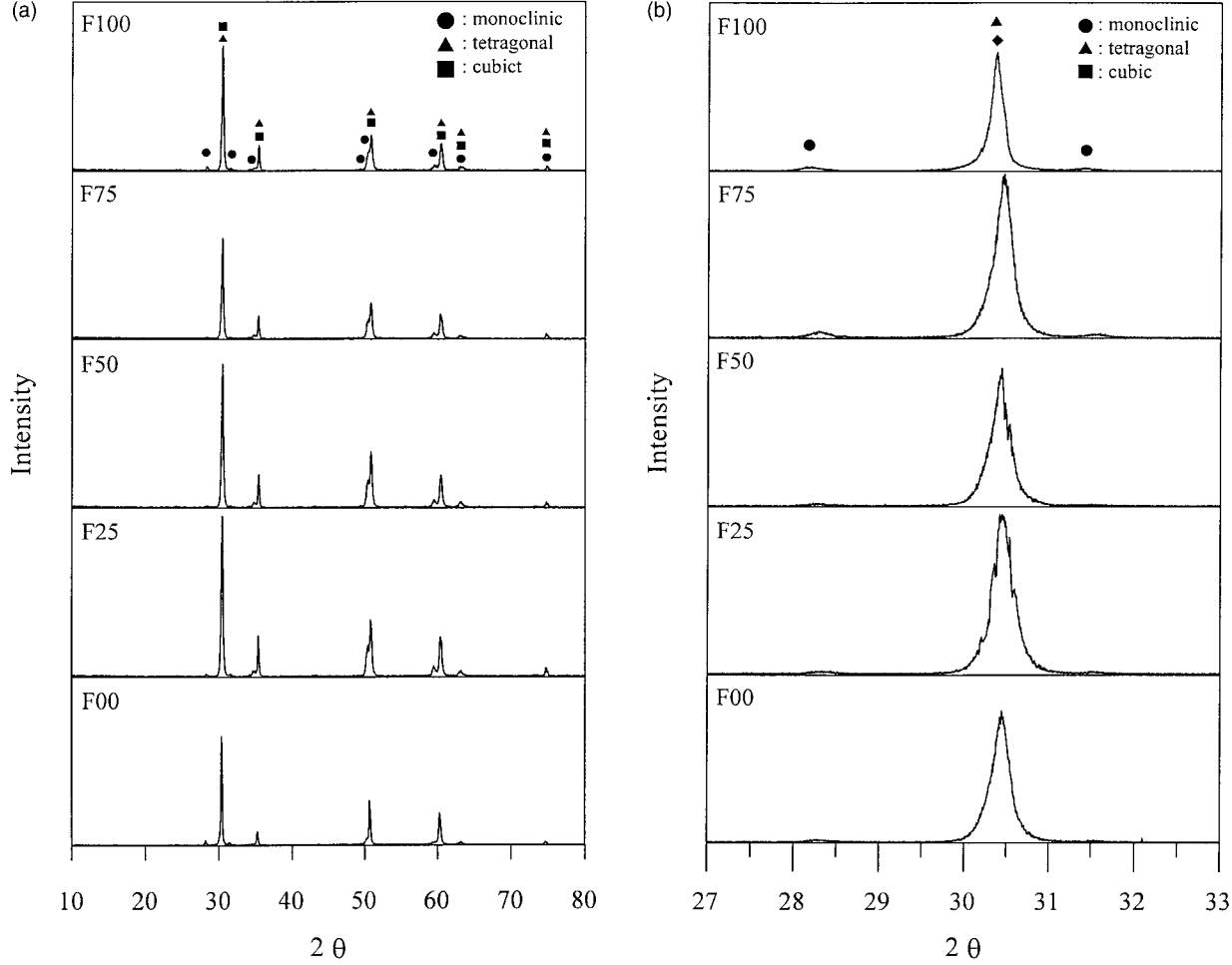


**Fig. 12.** (a) X-ray diffraction pattern between 10 and 80° two-theta angle of the sintered samples fired at 1650°C for 1 h. (b) X-ray diffraction pattern between 27 and 33° two-theta angle.

amount of m-phase is quantified to be $5 \pm 1\%$ for five zirconia samples. Then the added MgO stabilizes the zirconia prepared by injection molding and sintered at 1650°C quite well.

## 4 Conclusion

Five series of MgO–PSZ were prepared by the injection molding technique. The properties of feedstocks, green IM parts and fired pieces were investigated with respect to the size grading of the fine/coarse powders. The results appear that the flow behavior and the homogeneity of feedstocks and IM parts are closely relate to the ratio of coarse/fine powder in formulation. By using size grading, various types of zirconia parts can be made. The details of the results can be concluded as below.

1. The flowing behavior of the feedstocks is pseudoplastic. The flow index ($n$) and viscosity parameter ($k$) are controlled by the size grading of fine/coarse powders and the molding temperature.
2. The activation energy of the plastic feedstocks indicated that the temperature dependence of these formulations with $\geq 50\%$ coarse powder is similar to the binder. Their activation energies are in the range of 13 to 17 kJ $mol^{-1}$. However, the others with $> 50\%$ fine powder show a higher activation energy.
3. The content of fine powder helps the de-polymerization of PP ingredient and makes the decomposition reactions take place over a wider temperature range from 180 to 400°C.
4. The injection conditions were mainly controlled by the viscosity of the feedstocks and the content of fine powder. Green density, degree of debinding are in good control and the variation of these properties is less for formulations with a higher content of fine powder.
5. Porosity in the solvent debinded samples is widely distributed ranging from 0·01 to 1·00 $\mu$m. The size of the pores in the thermally debinded samples exhibits a normal distribution which corresponds to the interstitial space of each powder mixture.

6. The MgO–PSZ was densified to the relative density ranging from 60 to 93%. The higher the volume fraction of fine powder, the higher the density of the PSZ. The content of fine powder in the size-graded zirconia is the major decisive factor to the fired density of the PSZ.
7. There is no pure MgO or magnesium zirconate phase left in the 1650°C fired samples and the amount of monoclinic phase is about 5%.


## Acknowledgements

The authors gratefully acknowledge the support of the Tjing Ling Industrial Research Institute (85-G-14) and National Science Council (NSC85-2622-E-002-020).


## References


1. Colin, S., Jeannot, F., Dupre, B. and Gleitzer, C., Ceria-doped zirconia-graphite as possible refractory for tundish nozzles in steelmaking. *Journal of the European Ceramic Society*, 1993, **11**, 515–521.
2. Bullard, R. L. and Cheng, P. C., Long term casting with zirconia nozzles. *Iron and Steelmaking*, 1992, 19–26.
3. Gunn, D. A., Use of Experimental zirconia tundish nozzles in steel making. *Brit. Ceram Trans. J.*, 1991, **90**, 21–24.
4. Kienow, S., Refractory materials. *Ceramic monograph. Interceram*, 1979, **28**(3), 1–18.
5. Lutz, H. E., Swain, V. M. and Claussen, N., Thermal shock behavior of duplex ceramics. *J. Am. Ceram. Soc.*, 1991, **74**, 19–24.
6. Hunt, K. N. and Evans, J. R. G. and Woodthorpe, J., On the role of coupling agents in zirconia–polypropylene suspensions for ceramic injection molding. *Polymer Eng. and Sci.*, 1988, **28**(23), 1572–1577.
7. Sunil Kumar, C., Balagopal, N., Pai, B. C., Damodaran, A. D. and Warrier, K. G. K., Injection moulding of ceria–zirconia powder mixtures using an aqueous HPMC-PVA binder system. *Brit. Ceram. Trans., J.*, 1994, **93**, 53–56.
8. Bhaduri, S. B., Chakraborty, A. and Janardhana Reddy, J., Injection moulding of ceria-stabilized tetragonal zirconia polycrystals (Ce-TZP). *J. Mater. Sci. Let.*, 1990, **9**, 209–210.
9. de With, G. and Witbreuk, P. N. M., Injection moulding of zirconia (Y-TZP) ceramics. *J. Eur. Ceram. Soc.*, 1993, **12**, 343–351.
10. Allaire, F., Marple, B. R. and Boulanger, J., Injection molding of submicrometer zirconia: blend formulation and rheology. *Ceram. Intern*, 1994, **20**, 319–325.
11. Wei, W. and Lin, Y. P. Mechanical and thermal shock properties of size grading MgO–PSZ refractory, in preparation.
12. Lin, Y. P., Investigation on injection molding process and mechanical properties of zirconia with size grading. Master thesis, National Taiwan University, 1977.
13. Brydson, J. A., *Flow Properties of Polymer Melts*, Iliffe, London, 1970.
14. Garvie, R. and Nicholson, P. S., Phase analysis in zirconia systems. *J. Am. Ceram. Soc.*, 1972, **55**, 303–305.
15. Chong, J. S., Christiansen, E. B. and Baer, A. D., *J. Appl. Polym. Sci.*, **15**, 1971, 2007–2021.
16. Wei, W. J., Tsai, S. J. and Hsu, K. C., Effects of mixing sequence on alumina prepared by injection molding, *Journal of the European Ceramic Society*, (1998).
17. Edirishinghe, M. J., The effect of processing additives on the properties of a ceramic–polymer formulation. *Ceram. Int*, 1991, **17**, 89–96.
18. Edirishinghe, M. J., Shaw, H. M. and Tomkins, K. L., Flow behavior of ceramic injection molding suspensions. *Ceram. Int*, 1992, **18**, 193–200.